Lab on a Chip

Cite this: DOI: 10.1039/c1lc20014c

www.rsc.org/loc

PAPER

Axon diodes for the reconstruction of oriented neuronal networks in microfluidic chambers†

Jean-Michel Peyrin,‡*[a] Bérangère Deleglise,‡[a] Laure Saias,‡§[c] Maéva Vignes,[ac] Paul Gougis,[c] Sebastien Magnifico,[a] Sandrine Betuing,[b] Mathéa Pietri,[a] Jocelyne Caboche,[b] Peter Vanhoutte,[b] Jean-Louis Viovy*[c] and Bernard Brugg*[a]

Received 9th January 2011, Accepted 31st May 2011
DOI: 10.1039/c1lc20014c

Various experimental models are used to study brain development and degeneration. They range from whole animal models, which preserve anatomical structures but strongly limit investigations at the cellular level, to dissociated cell culture systems that allow detailed observation of cell phenotypes but lack the highly ordered physiological neuron connection architecture. We describe here a platform comprising independent cell culture chambers separated by an array of "axonal diodes". This array involves asymmetric micro-channels, imposing unidirectional axon connectivity with 97% selectivity. It allows the construction of complex, oriented neuronal networks not feasible with earlier platforms. Different neuronal subtypes could be co-cultivated for weeks, and sequential seeding of different cell populations reproduced physiological network development. To illustrate possible applications, we created and characterized a cortico-striatal oriented network. Functional synaptic connections were established. The activation of striatal differentiation by cortical axons, and the synchronization of neural activity were demonstrated. Each neuronal population and subcompartment could be chemically addressed individually. The directionality of neural pathways being a key feature of the nervous system organization, the axon diode concept brings in a paradigmatic change in neuronal culture platforms, with potential applications for studying neuronal development, synaptic transmission and neurodegenerative disorder such as Alzheimer and Parkinson diseases at the sub-cellular, cellular and network levels.

Introduction

The brain is an exquisitely complex structure, comprising many different interconnected neuronal areas in which each neuron makes hundreds to thousands of specific connections with nearby and remote cognate neurons. Various experimental models are used to study brain development and/or degeneration. These models range from whole animal models, in which the anatomical structures are intact but experimentation at the cellular level is severely restricted, to dissociated cell culture systems allowing fine observation of cell phenotypes but lacking the highly ordered connectivity of neurons in the brain. *In vitro* studies of neuronal connections have generally been limited to observations of small numbers of cells in dissociated two-dimensional (2D) cultures with random connections, or in slice cultures, in which connections follow 3D intermingled networks that vary from one sample to the other, and are partly severed by the slicing process. In addition, these standard cell culture systems cannot be used to study the spatial compartmentalization of neuronal signals. Two major technical issues have been hampering the elucidation of axonal and synaptic differentiation and degeneration: first, a separation of soma from neuronal endings is a prerequisite for studying local molecular mechanisms in different sub-cellular compartments; second, it was not possible so far to create oriented neuronal networks involving different neuronal subtypes.

Microfluidic techniques, exploiting microfabrication technologies and the physical properties of flows at the micron scale, are powerful tools for studying living cells.[1] Notably, microfluidic devices allowing the physical separation of soma from axons, thanks to micro-channels, were used to study neuronal cell behavior.[2–4] This type of system allows

[a]*Laboratoire de Neurobiologie des Processus Adaptatifs, CNRS, UMR7102, Université Pierre et Marie Curie, Paris, France. E-mail: jean-michel.peyrin@snv.jussieu.fr; Fax: +33 1 44 27 26 69; Tel: +33 1 44 27 32 42; bernard.brugg@snv.jussieu.fr*
[b]*Physiopathologie des Maladies du Système Nerveux Central, CNRS, UMR7224, INSERM UMRS 952, Université Pierre et Marie Curie, Paris, France*
[c]*Marcomolecules and Microsystems in Biology and Medicine, Institut Curie, Centre National de Recherche Scientifique, Université Pierre et Marie Curie, UMR 168, 75005 Paris, France. E-mail: jean-louis.viovy@curie.fr; Fax: +33 1 40 51 06 36; Tel: +33 1 56 24 68 45*
† Electronic supplementary information (ESI) available. See DOI: 10.1039/c1lc20014c
‡ Authors equally contributed to the work.
§ Current address: Cell and Developmental Biology, Centre for Genomic Regulation, 08003 Barcelona, Spain.

pharmacological intervention focused on axons or neuronal somas of a single neuronal subtype. However, accurate reconstruction of oriented neuronal networks with a connectivity similar to that formed *in vivo* by neurons originating from distinct brain structures was not possible because neurons seeded in both cell culture chambers send their axons to the respective opposite chamber.[5]

Here, we propose a microfluidic system allowing the reconstruction of oriented neuronal networks involving several different neuron populations with a predefined connection architecture and a specific fluidic access to various cellular subcompartments within these networks. The key innovation of this system is the presence of asymmetrical micro-channels that can be penetrated by axons in a single direction, separating two individual chambers (or more). This asymmetrical geometry operates as a directionally selective filter for axons and as an impermeable barrier for cell bodies. It functions as a "diode" for axonal projections. We seeded primary neuronal cultures in this directional system, reconstituted cortico-striatal projections, and demonstrated the formation of active neuronal connections. *In vivo*, the striatal neurons present in the neostriatum are the principal recipients of glutamatergic cortical afferents (fibers of axons issued from cortical neurons) from the basal ganglia.[6,7] Using immuno-cytochemistry and functional analysis we showed that cortical fibers trigger full differentiation of medium spiny neurons (neurons contained in the receiving chamber, which were only partly differentiated before the arrival of cortical axons), with extensive formation of dendritic spines (a morphological signature of neuronal connections) and functional glutamatergic cortico-striatal synapses. This leads to the creation of an integrated binary neuronal network that fully mimics the *in vivo* neuronal pathway, opening the route to a number of applications ranging from developmental neurosciences to neuropharmacology. We finally discuss the generality of this platform and its potential for studying localized degenerative events at the cellular and subcellular levels in various neurodegenerative diseases, or for studies of physiological brain development and neuronal communication.

Results

Set up of an oriented microfluidic cell culture system allowing directional axonal outgrowth

Our microfluidic neuron culture platform involves two main features. The first one is the culture of two (or more) cell populations in microfluidic chambers, connected by an array of microstructures allowing axonal communication between these chambers without mixing soma. This system was inspired from Taylor *et al.*[3] The second one is a new and original approach to reproduce the directionality of neuronal connections observed *in vivo*, a critical parameter for efficient neuronal functioning. Previous studies have shown that axonal growth can be controlled by mechanical constraints[8,9] and that axons tend to follow straight microfluidic structures, a property previously used by Jeon's Lab[3] to separate, in two distinct chambers, axonal endings from neuronal somas (Fig. 1a). In an effort to optimize the microstructures allowing crossing and invasion of the axonal chamber, we used a multi-dimensional chip comprising 2 distinct cell culture chambers separated by arrays of rectangular micro-channels of decreasing width (Fig. 1b). As shown in Fig. 1c, the number of axons per channel is highly correlated to the width of the channels. Whereas large micro-channels, 20 to 15 μm wide, allow a complete invasion of the distal chamber with 15 to 20 axons per channel, decreasing the width reduces the number of axons entering the channels. For really narrow (<3 μm) and long micro-channels axonal length and integrity are reduced. Moreover we observed that axons encountering a wall perpendicularly deviate, whereas axons encountering a wall tangentially continue growing along the wall.

We tried to exploit these properties to impose a directionality that would allow axons to grow only from one chamber (emitting) to the other (receiving) and not the opposite way. Based on the effect of width of rectangular micro-channels on axonal crossing (Fig. 1b), we designed asymmetrical funnel-shaped micro-channels (named "axon diodes"). The resulting oriented microfluidic cell culture comprises two distinct cell culture chambers (Fig. 2a), each connected to two reservoirs and

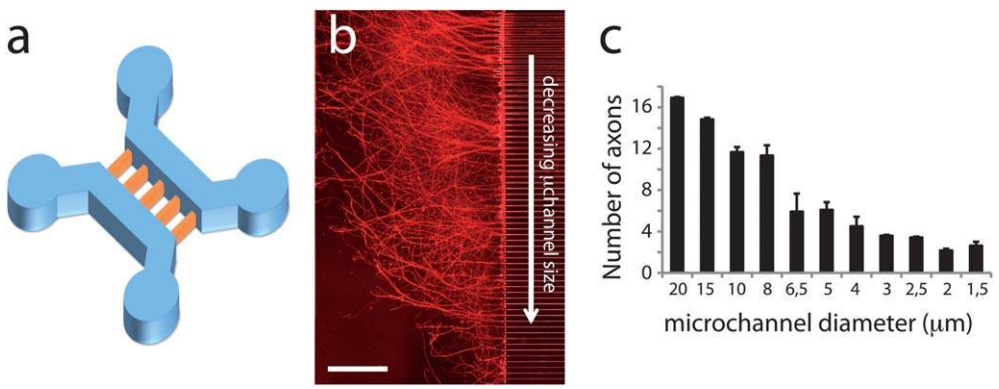

Fig. 1 *Effect of the width entrance of rectangular straight channels on axonal crossing.* (a) The microfluidic neuronal culture devices derived from ref. 3 are composed of two separate cell culture chambers separated by an array of rectangular micro-channels (500 μm long, 3 μm high) with eleven variable width ranging from 20 to 1.5 μm by groups of 6 identical micro-channels per width. (b) Primary cortical neurons seeded in a multidimensional microfluidic chip with variable width ranging from 20 to 1.5 μm. 10 days after cell seeding, the axonal chamber was immuno-stained for tubulin. (c) Quantification after 10 days of culture, of the number of axons exiting the micro-channels.

separated by a series of 500 μm long, 3 μm high, asymmetrical micro-channels (Fig. 2b). Based on Fig. 1c we chose a 15 μm entrance allowing optimal axonal collection from the emitting chamber. As shown in Fig. 2c, when seeded in the chamber on the wider ("emitting") side of the axon diodes, mouse primary cortical neurons emit axons; their entrance into the micro-channels being facilitated by the large openings. Axons that have entered a micro-channel tend to fasciculate and grow in bundles; they do not stop in the narrowing section, guided by the channel walls. In order to assess whether the funnel like channel causes axonal "engorgement", we then tested the influence of the narrowest side width on axonal crossing. In comparison to a 15 μm wide rectangular channel, 15 to 5, 3 or 2 μm wide diodes allowed 90%, 70% and 30% respectively of receiving chamber invasion (not shown). Using a 15 to 3 μm diode, 8 days after cell seeding, the "receiving" (narrow side of the channel) chamber is massively invaded by axons which de-fasciculate and branch 50 to 100 μm after exiting the micro-channels (Fig. 2c).

In contrast, when neurons are seeded at the same density in the "receiving" chamber, the number of axons reaching the opposite chamber is greatly reduced (Fig. 2d). Axons tend to bump into the sidewall of the cell culture chamber and keep their new directionality by following the wall of the receiving chamber without entering the narrow micro-channels (only a small fraction is able to enter the micro-channel "tips"). The relative amount of axon projections from both sides was quantified for an optimal width of micro-channel tips. For 15 μm wide openings on the emitting side and 3 μm wide on the receiving one, the number of axons projected with the "forbidden" polarity (*i.e.* from the narrow side to the wide side) was only around 3 to 5% of the number of axons projected along the allowed polarity (Fig. 2e).

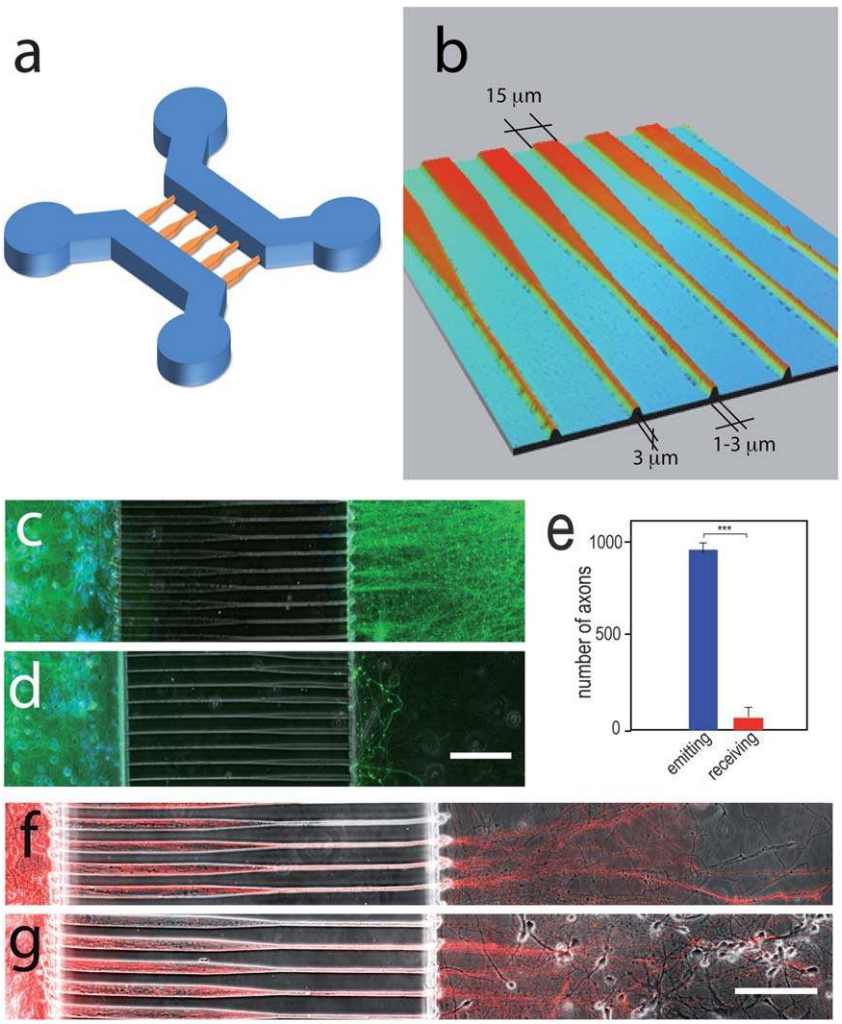

Fig. 2 *In vitro reconstruction of a neuronal network using "axonal diodes" in microfluidic culture devices.* (a) Global 3D view of the microfluidic device comprising asymmetrical microchannels (b) 3D view of the funnel-shaped micro-channels as observed by white-light optical profiling (WLOP) with an interference microscope. Immunofluorescent images of microfluidic cultures (green: α-tubulin, blue: Hoechst) in which cortical neurons were seeded either on the wide (c, 15 μm) or the narrow (d, 3 μm) side, at a concentration of 45×10^6 cells per ml. Note the lack of labeling in the wide chamber when cortical neurons are seeded in the narrow side (d). (e) Quantification showing that the axonal diodes efficiently polarize axonal growth (*** p-value < 0.001). Phase contrast image combined with epifluorescence of a reconstructed polarized neuronal-network after 8 days *in vitro*. To visualize individual axons of cortical neurons, cells were transduced with a m-cherry Sindbis viral vector (red). Cortical neurons projecting their axons into the second chamber without a target (f) or in the presence of striatal neurons seeded in the second chamber (g). Note that striatal neurons are not infected by the virus, indicating an effective compartmentalization of the two culture chambers. *Scale bar 50 μm.*

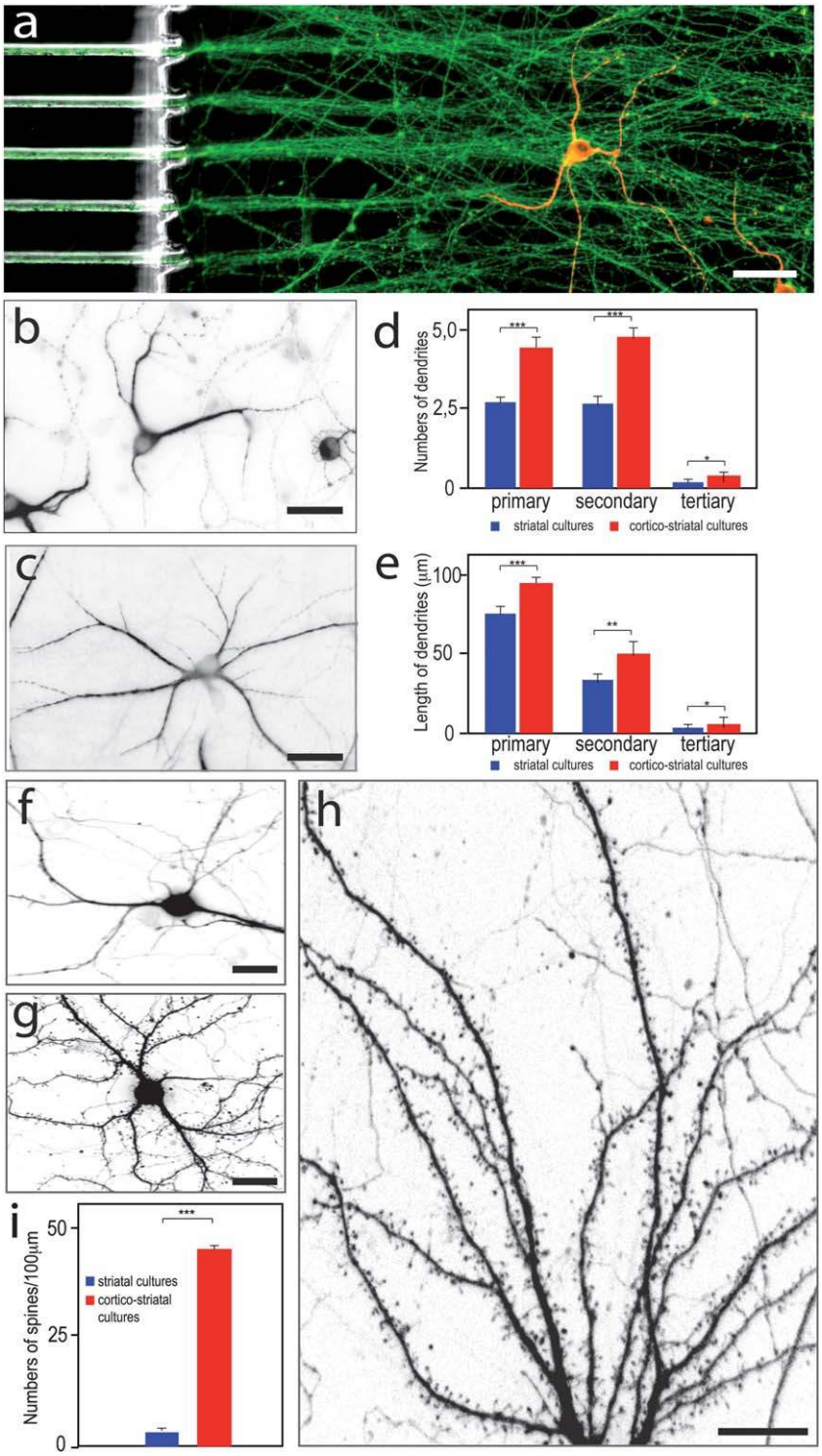

Fig. 3 *Cortical afferents promote striatal neurons differentiation.* (a) Dendritic MAP-2 immuno staining (red) of striatal neurons (13 DIV) receiving cortical afferents (in green, α-tubulin). Morphological analysis of striatal neuron arborization using MAP-2 immunolabeling in the absence (b) or presence of cortical afferents (c). Quantification of the number (d) and length (e) of striatal neuron dendrites. (d) *p*-Value: primary = 5.5×10^{-4}, secondary = 5.5×10^{-3}, tertiary = 9.6×10^{-3}. (e) *p*-value: primary = 3.9×10^{-5}, secondary = 2.1×10^{-5}, tertiary = 4.6×10^{-2} ($n = 40$ neurons per condition (3 independent experiments). (f–h) Images of GFP-expressing striatal neurons. Striatal dendrites receiving afferents from cortical neurons have many more dendritic spines (g and h) than those cultured alone (f). (i) Quantification of spine density (per 100 µm) in GFP positive striatal dendrites grown in the presence and absence of cortical afferents (***p-value < 0.001). *Scale bar: 50 µm.*

Establishment of an oriented neuronal network

We then reconstructed oriented neuronal cortico-striatal projections. Primary cortical neurons from the neocortex were seeded on the emitting side of the diodes, and striatal neurons from the same mice were seeded on the receiving side. Immunocytochemical analysis shows that cortical cells are composed of 90% MAP2 positive neurons among which 5 to 10% are GAD67 inhibitory interneurons and around 90% are VGLUT1 glutamatergic neurons. After two weeks in culture, striatal cells seeded in the receiving chamber are composed of 80% neurons among which 90% are GAD67 positive inhibitory neurons (ESI, Fig. S2†). Fig. 2f shows phase contrast micrographs of cortical neurons projecting their axons through the axonal diodes and connecting to the striatal neurons in the receiving chamber after 8 days in culture (Fig. 2g). To distinguish cortical axons growing in the striatal chamber from striatal axons and dendrites, cortical neurons were transduced after 7 days in culture in the emitting chamber, with a Sindbis viral vector encoding m-cherry fluorescent protein. The viral vector transduced up to 80% of cortical neurons. Their axons projecting in the receiving chamber were stained in red and easily discriminated from unlabeled striatal axons and dendrites (Fig. 2f and g). These axons established contacts with striatal neurons and continued to grow across the receiving chamber suggesting the formation of "en passant" connections as those observed *in vivo* in the cortico-striatal pathway. The oriented network in the diode devices was maintained routinely for 3 weeks *in vitro*, thus allowing short and long-term experiments.

Cortical fibers establish synaptic contacts with striatal dendrites and induce spinogenesis and striatal maturation

Having shown that cortical axons invade the receiving chambers we tested whether the presence of cortical fibers in the receiving chamber affected striatal differentiation. After 15 days *in vitro*, cells were fixed and immunostained for MAP-2 to evaluate the degree of striatal neuron arborization (Fig. 3a). Pure striatal cultures present many immature-like neurons, as compared to the numerous mature-like multipolar neurons with extended processes found in cortico-striatal co-cultures (compare Fig. 3b and c). Morphometric analysis on striatal neurons grown alone or in the presence of cortical afferents showed that the former had in average 3 primary (starting from the soma) and secondary dendrites (starting from primary dendrites) and no tertiary dendrites per cell, whereas the latter had in average 4 primary, 5 secondary and 1 tertiary dendrites after 2 weeks in culture (Fig. 3d). The dendrites of striatal neurons grown in the presence of cortical axons were also significantly longer (Fig. 3e). Interestingly this differential maturation is exacerbated after 3 weeks in culture as shown in Fig. 3f–g. Another morphological consequence of the presence of cortical afferents on the formation of striatal dendritic spines was revealed by culturing striatal neurons from transgenic mice expressing GFP (green fluorescent protein) under the control of an actin promoter in all cell types. GFP positive striatal dendrites grown in the presence of cortical afferents had many dendritic spines (40 spines per 100 μm) whereas striatal neurons cultured alone were virtually devoid of spines (2 spines per 100 μm) (Fig. 3f–i). These findings indicate that cortical fibers coming from the emitting chamber promote striatal differentiation *in vitro* in the receiving chamber.

To confirm that cortical fibers form synapses on striatal dendrites, neurons were stained for the pre- and postsynaptic markers VGLUT1 and PSD-95, respectively. Whereas both VGLUT1 (Fig. 4b) and PSD-95 (Fig. 4d) show faint and sparsely clustered signals on unconnected cortical fibers or single striatal neurons, respectively, cortico-striatal projections (Fig. 4a and c) led to a dramatically increased labeling of the presynaptic markers along cortical axons, with dense clustering of VGLUT1 (Fig. 4a, inset a′), and clustering of the post-synaptic marker PSD95 (Fig. 4c, inset c′ and c″) along the MAP-2 positive striatal dendrites. Co-localization experiments showed that presynaptic cortical VGLUT1 staining is present on top of the GFP positive striatal dendritic spines apposing to postsynaptic PSD-95 positive striatal structures (arrow heads, Fig. 4e).

Functionality of the cortico-striatal synapses

We next assessed whether the synapses of the cortico-striatal network were active. Striatal neurons are GABAergic neurons expressing various glutamate receptor subtypes including members of the NMDA receptor subfamily. Electrical stimulation of the glutamatergic cortico-striatal pathway triggers a phosphorylation cascade leading to the activation of the Extracellular-signal Regulated Kinase (ERK).[10] Immuno-cytochemical detection of phosphorylated ERK (P-ERK) in striatal neurons shows that approximately 15% of striatal neurons cultured alone exhibit robust P-ERK cytosolic staining (Fig. 5c). However P-ERK staining increases to 30% when grown in contact with cortical fibers, indicating that cortico-striatal connections induced a basal ERK activation (Fig. 5a and b). When the cortical emitting compartment was stimulated with KCl, to depolarize cortical neurons, the proportion of striatal neurons showing P-ERK staining increased to 60% (Fig. 5c). This activation was partially inhibited by incubation with the glutamatergic NMDA receptor (NMDAR) antagonist MK801, within the receiving striatal chamber (Fig. 5c). A Fluo4 non-ratiometric calcium analysis of primary neurons (Fig. 6) revealed that cortical neurons progressively show spontaneous slow calcium oscillation reminiscent of intrinsic cortical connectivity (Fig. 6a–c). After 12 to 16 days *in vitro*, approximately 50 to 70% of cortical neurons exhibit synchronous calcium oscillation (Fig. 6c), while when grown alone, striatal cells never show any sign of calcium oscillation (Fig. 6d). In contrast, striatal neurons connected to cortical fibers acquire spontaneous slow calcium oscillation in synchrony with cortical fibers (Fig. 6e), a process abolished by striatal MK801 (Fig. 6f) or TTX (Fig. 6g) application.

In summary, our system allows the reconstruction of an oriented and fully mature cortico-striatal neuronal network, in which post-synaptic neurons are functionally connected to glutamatergic cortical fibers.

Discussion

Advantages of microfluidic axonal diodes for neuronal network reconstruction *in vitro*

During the last few years, microfluidics has brought new perspective in the development of models in cell biology. Several systems have been proposed to reconstruct neuronal networks.[11–14] Relatively

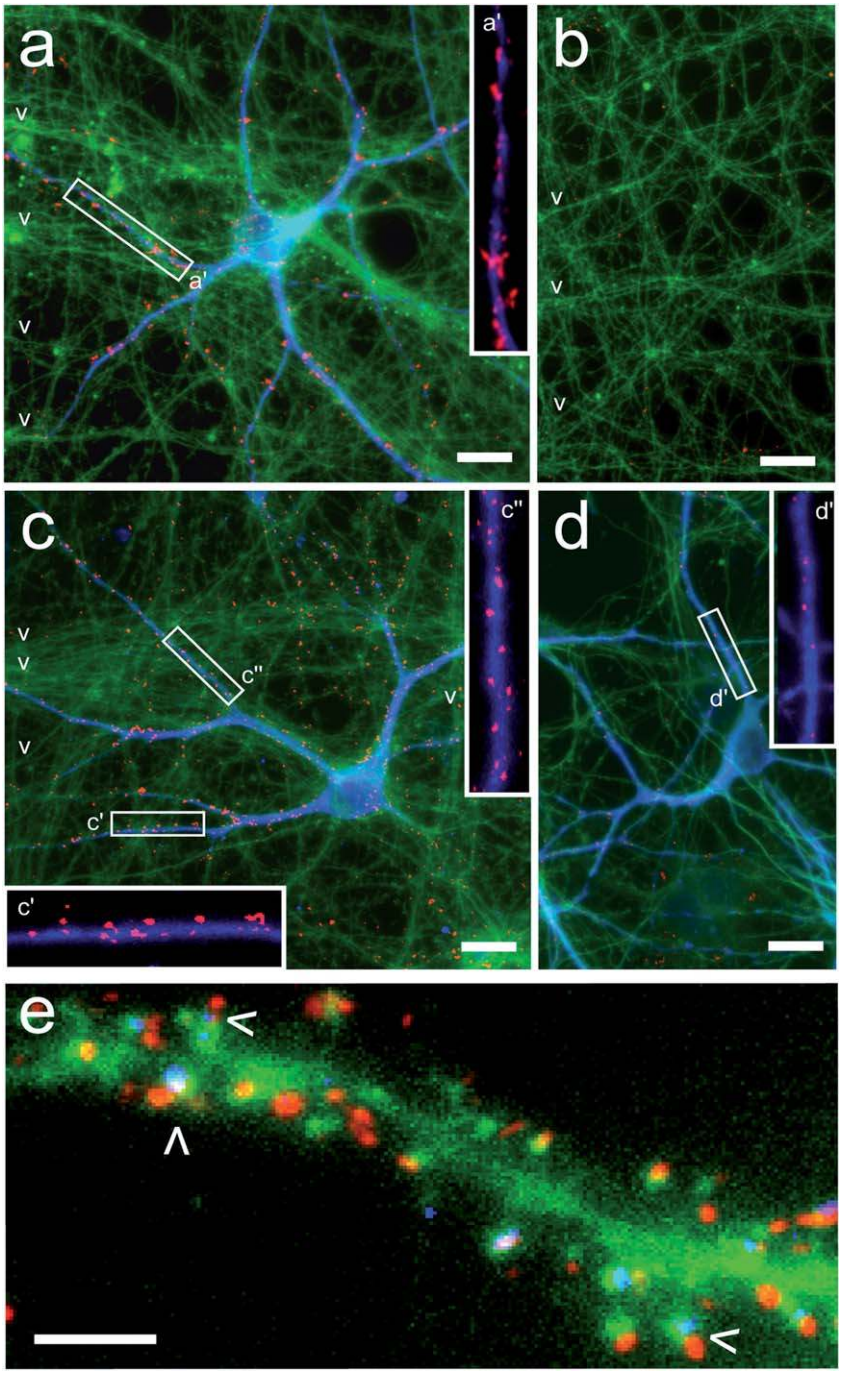

Fig. 4 *Cortico-striatal microfluidic co-culture enhances synaptic maturation*. (a and c) Striatal cultures in the presence of cortical fibers. Neurons in the striatal chamber were immunocytochemically labeled for MAP-2 (blue), and afferents from cortical neurons for α-tubulin (green, arrowheads). VGLUT1 (red) (a and b) and PSD95 (red) (c and d) were used as pre- and post-synaptic markers, respectively. (b) Cortical axons cultured in the absence of striatal neurons. Note that cortical neurons present scarce and dispersed VGLUT1 clusters on their axons, reminiscent of partial maturation of presynaptic terminals. (d) Striatal neurons cultured alone present sparse clusters of PSD-95 indicating an intermediate state of differentiation of striatal neurons. The greater VGLUT1 (a) and PSD95 (b) staining and clustering are observed especially where cortical axons and striatal neurons seem to connect, reminiscent of synaptic protein relocalization to cortico-striatal contacts. a′, c′, c″and d′: higher magnification of the synaptic markers (red) on striatal dendrites (blue). Co-localization experiments showed that presynaptic VGLUT1 staining is present on top of the GFP positive striatal dendritic spines apposing to postsynaptic PSD-95 positive striatal structures (e). *Scale bar: 10 μm*.

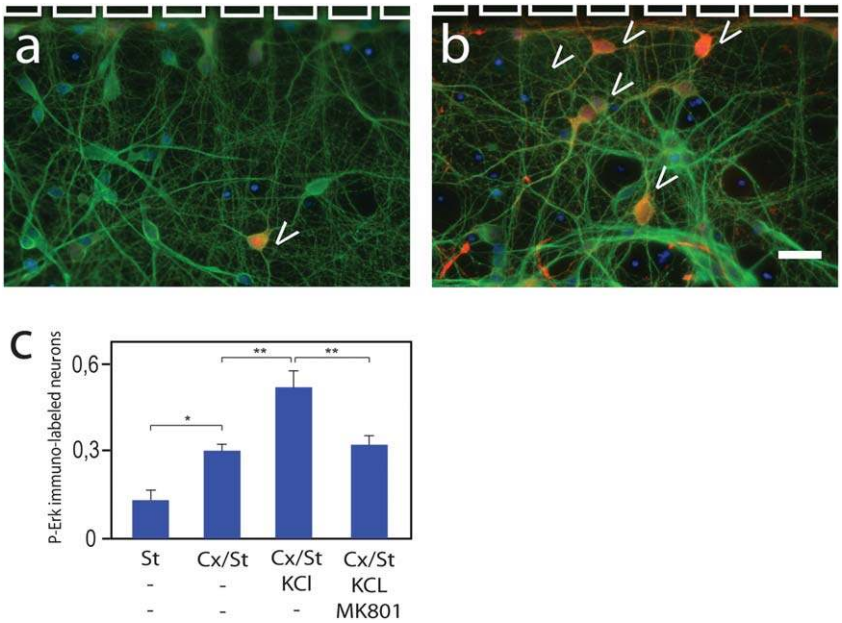

Fig. 5 *Cortical depolarization induces glutamatergic neurotransmission and subsequent ERK activation.* Cortico-striatal networks were grown for 12 to 14 days *in vitro*. ERK activation was analyzed in striatal neurons by immunocytochemical detection of its phosphorylated form (P-ERK, red): P-ERK labeling in striatal neurons (arrowheads) in basal conditions (a) and 20 min after a stimulation of the cortical somato dendritic compartment with KCl (50 mM) (b). (c) P-ERK signal was counted in 3 independent experiments before and after KCl treatment, in the presence and absence of MK801, a selective NMDA glutamate receptor antagonist (* p-value < 0.05, ** p-value < 0.01). *Scale bar: 20 μm.*

simple microfabrication tools can be used to spatially isolate the soma of a CNS neuron from its axons and axon-terminals.[2,3] Using such systems Taylor *et al.* showed that microfluidic channels allow fine manipulation of hippocampal auto-synapses.[5] In the brain, however, different neuronal populations are connected with well-defined topologies and polarities. Directionality is at the heart of developmental mechanisms involved in the specific connection of different neuronal subtypes. It is also critically involved in the degeneration of neuronal networks in mature brains. Today, no system is able to model a directional network comprising distinct neuronal sub-population so far. In order to obtain directional networks *in vitro*, distinct approaches can be envisioned including axonal mechanical constraints and/or combination of specific gradients of axonal growth cones attractant/repellent. We chose to use physical constraints because their efficiency should not depend on the neuronal type, allowing the use of the same microfluidic system for all neuronal subtypes. The axonal diode concept overcomes the limitation of previous non-polarized systems, allowing a good selectivity towards the allowed connection direction.

The polarity is maintained over time due to several complementary effects (Fig. S1†): first asymmetry imposes directionality by a probabilistic effect, easing the entrance of axons on the wide side of the diode in comparison to the narrowest side. Moreover, we observed that axons from neurons, seeded in the receiving chamber, once encountering the diode wall instead of the micro-channels entrance tend to grow perpendicularly to the diode along the chamber wall, without entering to a great extent the narrow side of the diodes. This effect is probably due to axonal stiffness that prevents frequent axonal turning. Indeed, we noticed that once guided by a parallel microstructure, axons tend to keep that direction for 50 to 100 μm once exiting the microstructure. Thus axons encountering a perpendicular wall will turn and keep the new direction. Finally, once emitting axons enter the receiving chamber it is likely that a second filtering effect occurs *via* steric hindrance of the micro-channels that have been filled. Therefore these complementary effects allow a long lasting polarity.

Technically, this system involves a moderate increase in the difficulty of microfabrication; it requires more care and resolution due to the smaller size of the structures, but it remains within the scope of standard microfabrication clean rooms. Indeed, as proposed in the Experimental section, the use of a polymer resin secondary master made from a primary silicon template further increases fabrication simplicity and can be used for years. This way, once a primary master has been prepared, hundreds of microfluidic chips can be prepared without a clean room, directly in the biology lab if necessary.

The directionality of neuronal pathways being a key feature of the nervous system organization, the axon diode concept brings a paradigmatic change in the potential of microfluidic neuron culture platforms for biological studies. Reconstructing a fully mature, functional and oriented neuronal network, in which each cell population and subcellular compartment can be addressed independently, is an important step in bridging the gap currently separating *in vivo* and *in vitro* studies. While *in vivo* studies are indisputably realistic regarding neuronal architectures, they remain very limited for studying molecular and cellular mechanisms. In contrast, *in vitro* studies performed so far allowed molecular and cellular investigations, but lacked a physiologically realistic connectivity. Our microfluidic platform reconciles these two concerns by giving access to precise cellular and molecular dissections in a physiological context.

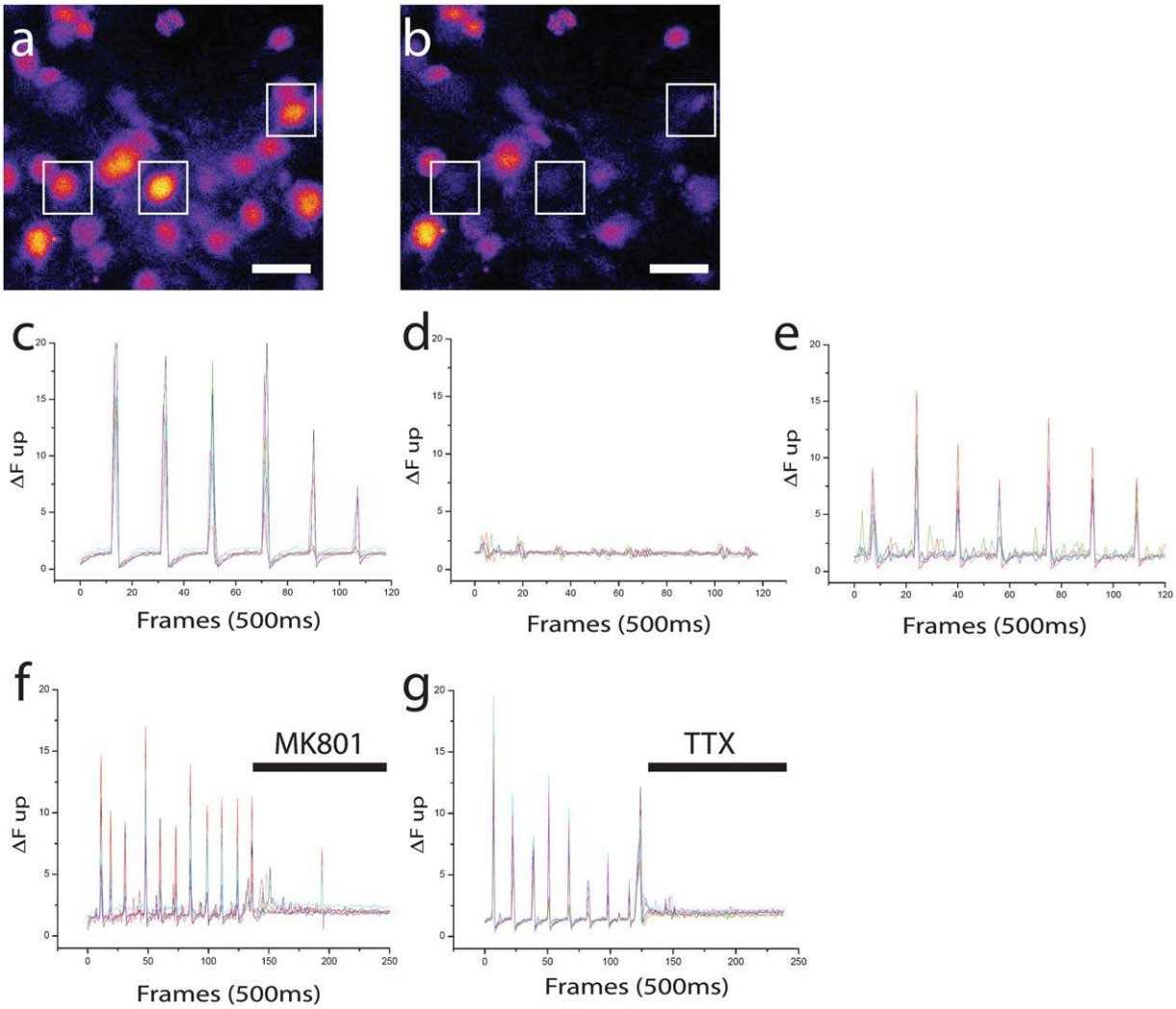

Fig. 6 *Striatal neurons acquire slow calcium oscillation*. (a and b) Snapshot of Fluo4 oscillation of 15 days old cortical cultures (40× magnification, pseudo colors: (a): up, (b): resting). 50% of cortical neurons shows synchronous sign of oscillation. Representative calcium traces analysis of 15 days old, cortical neurons (c), unconnected striatal neurons (d), connected striatal neurons (e). Connected striatal neurons before and after 10 μM MK801 striatal perfusion, (f), connected striatal neurons before and after 1 μM TTX striatal perfusion (g). Fluo4 signal oscillations of individual cells from the same experiment were plotted on the same graph.

Reconstruction of a physiologically active network and its importance for neuronal differentiation

As a proof of concept, we reconstructed *in vitro* the cortical–striatal neuronal pathway. The striatum is the principal component of the basal ganglia, which is composed of the caudate, putamen, and accumbens nuclei. Basal ganglia form recurrent circuits critical for motivation and motor planning. The striatum receive glutamatergic inputs from both cortical and thalamic afferents and dopaminergic inputs from the substantia nigra in the midbrain.[6,7,15] Ninety to 95% of the striatal neurons are GABAergic inhibitory medium spiny neurons (MSN)[16] which have a medium-sized cell body with branched dendrites presenting a high density of dendritic spines. *Via* their projections, striatal neurons give rise themselves to a direct (striato-nigral) and an indirect (striatopallidal) pathway. One of the targets of these two pathways is the thalamus, which in turn sends axons to the cortex leading to a retro-control feedback loop. The activity of the striatum is mainly driven by excitatory connections coming from diverse areas of cerebral cortex, including sensory, motor and association regions that project to the striatum mainly through ipsilateral glutamatergic projections. This is a purely directional pathway in which the cortical fibers, originating from pyramidal neurons of the layer V, invade the striatum and connect striatal dendrites "en passant",[15] a single cortical axon connecting several striatal neurons. In our system, cortical fiber reconnection on striatal dendrites did trigger both presynaptic clustering along striatal dendrites and striatal neuron maturation. This involves an increase in striatal dendritic arborization complexity, PSD95 clustering and dendritic spine genesis. These observations are in line with previous studies showing that striatal differentiation is partially under the control of cortical neurons.[17] The examination of cortical fibers transduced by a Sindbis viral vector encoding the m-cherry fluorescent protein in cortical cells indicated that cortical axons, which are highly branched in our culture

conditions and grow over more than 2 mm, connect striatal dendrites on their way without stopping, a single cortical axon connecting several striatal neurons (Fig. 2g). This reproduces *in vivo* data on the establishment of "en passant" glutamatergic contacts between cortical axons and striatal neurons.[18] These uni-directional cortico-striatal connections were fully functional: the spontaneous slow calcium oscillation in the cortical population was transferred to the striatal one, whereas in the absence of connection with cortical axons, the striatal population did not show any oscillation. Furthermore, KCl-induced depolarization of cortical neurons reproduced ERK activation in striatal neurons, as observed *in vivo* after electrical stimulation of the cortico-striatal projections.[10] Thus our platform directs neuronal connections, allows separate labeling and stimulation of different cell populations, and allows the observation of various cellular subcompartments at high resolution.

Conclusions and perspectives

In this study we propose the concept of axonal diodes, allowing the *in vitro* reconstruction of oriented and compartmentalized neuronal networks with physiologically active synaptic connections mimicking *in vivo* architectures.

These experiments only represent a very small fraction of the potential applications of the *in vitro* reconstruction of polarized neuronal networks. For instance, more complex networks, involving 3 neuronal populations or more, will be at hand, thanks to a moderate increase in the complexity of the microchannels array set-up. An obvious application is the investigation of the molecular and cellular mechanisms underlying synaptic and neuronal dysfunction during Alzheimer's, Parkinson's and Huntington's diseases, or prion diseases.[19–21] Furthermore, this system is also a valuable tool to address developmental issues such as the dynamics of neural networks and synapse formation. Interestingly, too, it will allow the construction of neuron arrays imposing *ad hoc* non-physiological connectivities, providing additional levers to test biological hypotheses regarding *e.g.* neuron maturation and communication. Finally, the axon diodes microfluidic platform could easily integrate microelectrodes, and thereby its range of application could be extended to electrophysiology and cognitive sciences.

Experimental

Chip design and master fabrication

The microfluidic channels comprise two types of component: large channels (50 μm in height) for cell injection and thin channels (2 or 3 μm in height) for axon growth. To fabricate the template with elements of two different depths, we used two layers of photoresist (SU82002 and SY355). A silica wafer was heated to 150 °C and activated by plasma treatment (30 s). A first layer of SU82002 (Microchem) was spin-coated onto the wafer at 2000 rpm and then soft-baked at 65 °C for 2 min and 95 °C for 4 min. The template was then exposed to UV light through an optic mask (made of plastic or quartz if the required resolution was less than 8 μm). After hard bake, the channels (2–3 μm high) were developed in an SU8 developer. The injection channels were then fabricated by laminating the latter wafer with a 55 μm thick layer of dry film SY355 (Elga Europe) at 70 °C. A second mask was aligned over the SU8 channels and after exposure to UV light, the channels were baked for 5 min at 120 °C and developed in a BMR developer, then rinsed with BMR rinse and isopropanol.

The quality of the narrowing micro-channels was assessed by white-light optical profiling (WLOP) in the vertical scanning mode (VSI), with an interference microscope Wyko® NT1100 (Veeco Instruments Inc., Plainview, NY, USA). The 3D representation was obtained with a 50× magnification objective.

Silicon templates were replicated within a polyester resist (Dalbe), which is more robust than silicon wafers. These templates were fabricated by pouring a mixture of polyester base and curing reagent (2%) over a PDMS replica that was previously heated to 110 °C. The resist was cured at 110 °C for 20 min and then at 150 °C for at least 3 h. Two different microfluidic chips were constructed in this way. The first ("2C") is a two-compartment chip made of two rectangular macro-channels (length: 4000 μm; width: 500 μm; height: 55 μm) separated by arrays of asymmetrical micro-channels (length 500 μm, 15 to 3 μm width, 3 μm height; see Fig. 1 a–c).

Microfluidic chip production

PDMS (Sylgard 184) was mixed with curing agent (9 : 1 ratio) and degassed under vacuum. The resulting preparation was poured onto a polyester resin replicate and reticulated at 70 °C for 2 hours. The elastomeric polymer print was detached and 2 reservoirs were punched for each macro-channel. The resulting piece was cleaned with isopropanol and dried. The polymer print and a glass cover slip were treated for 1 minute in an air plasma generator (40% power, 300 mTor, Diener) and bonded together. Chips were placed under UV for 15 minutes and then coated with a solution of poly D-lysine (10 μg ml^{-1}) overnight and washed with PBS before cell seeding.

Primary neuronal cultures

Cortices and striata were micro-dissected from E14 embryos of Swiss mice (René Janvier, France) and of a transgenic mice strain expressing GFP (green fluorescent protein) under the control of an actin promoter in all cell types.[22] Animal studies were carried out in accordance with the standard ethical guidelines (European Community guidelines on the care and use of laboratory animals: 86/609/EEC). The laboratory animal facility was approved by prefectoral decision of the Bureau of Sanitary Police, Paris Prefecture, #DTPP 2010-1230, Nov. 4, 2010. All dissection steps were performed in cold PBS supplemented with 0.1% glucose. Dissected structures were digested with trypsin–EDTA (Gibco) and mechanically dissociated with a pipette. After several rounds of rinsing with phosphate-buffered saline (PBS), cells were re-suspended in DMEM, to a final density of 40 million cells per ml for cortices and 15 million per ml for striata. Cortical cells were then seeded in the somatic compartment and striatal cells in the distal compartment: 3 μl of the cell suspension was introduced into the upper reservoir and cells flowed into the chamber and adhered within 1–2 minutes. The cell culture medium was then added equally to the four reservoirs (40 μl/reservoir). Both neuronal cell types were grown in DMEM glutamax + streptomycin/penicillin (Gibco) + 10% FBS + N2 (Gibco) + B27

(Gibco). Microfluidic chips were placed in plastic Petri dishes containing H_2O–EDTA to prevent evaporation and incubated at 37 °C in a humid 5% CO_2 atmosphere. The culture medium was renewed every 3 to 5 days. Upon differentiation, 2 or 3 days after seeding, cortical axons entered the micro-channels and reached the second chambers after 4 to 5 days. Cortical axons continued growing thereafter. Flows were controlled by gravity pressure; each macro-chamber is connected to two reservoirs punched in a reproducible way, thus seeding these reservoirs with specific volume ensure control of flow rate for the desire amount of time.

Immunofluorescence

At various times, depending on the phenomenon under study, cultures were fixed in 4% paraformaldehyde (PFA) for 20 minutes at room temperature. Cells were then washed twice with PBS for 5 min and permeabilized for 45 min with 0.2% Triton X-100 and 1% BSA in PBS. Primary antibodies were then added and the samples incubated at 4 °C overnight in PBS. The samples were rinsed twice for 5 minutes with PBS and further incubated with the corresponding secondary antibodies for 2 hours at room temperature. The chips were then rinsed once with PBS and once with PBS + 0.1% sodium-azide and mounted in a mowiol mounting medium. The following primary antibodies were used: α or β3-tubulin-FITC (monoclonal 1/700, sigma); MAP-2 (mouse monoclonal 1/400, Sigma); synaptophysin (mouse monoclonal 1/400, Sigma); VGLUT1 (rabbit polyclonal 1/500, gift E. Herzog, CNRS, UMR 7224); PSD95 (rabbit polyclonal 1/200 cell signaling); GAD67 (mouse monoclonal 1/500, Millipore); Darpp32 (mouse monoclonal 1/500, gift J-A. Girault, Inserm, UMR-S839) and anti-phospho ERK antibodies (mouse monoclonal 1/1000, cell signaling). Species-specific secondary antibodies coupled to Alexa 350, 488, and 555 were used (1/500, Invitrogen) to visualize bound primary antibodies.

Neuronal network stimulation

To decrease serum-induced ERK activation, 13 to 15 day old pure striatal cultures or reconstructed cortico-striatal networks were serum starved for at least 6 hours. To stimulate cortical neurons, the cortical chamber was subjected to DMEM containing 90 mM KCl for 20 minutes. In some experiments, 10 μM MK801 was introduced into the striatal chambers prior to KCl stimulation. Cell cultures were then fixed with PBS containing 4% PFA and further processed for P-ERK or neuronal immunocytochemistry. To quantify ERK stimulation in striatal neurons, random fields of MAP-2 positive neurons apposed along cortical fibers were counted for phospho-ERK immunoreactivity. Reported values are means from three independent experiments each performed in triplicate.

Image acquisition

Images were acquired with an Axio-observer Z1 (Zeiss) fitted with a cooled CCD camera (CoolsnapHQ2, Ropert Scientific). The microscope was controlled with Metamorph software (Molecular Imaging) and images were analyzed using Image J software.

Non-ratiometric calcium analysis

After 12 to 16 days *in vitro*, micro-chambers were rinsed twice with loading buffer (NaCl 129 mM, KCl 4 mM, $MgCl_2$ 1 mM, $CaCl_2$ 2 mM, Glucose 10 mM, Hepes 10 mM dissolved in sterile water). Cells were then incubated for 30 min at RT, with 2 μM fluo4 calcium probe (Invitrogen) dissolved in loading buffer. After 2 rinses cells were returned in DMEM cell culture medium and recorded, at room temperature, under the microscope (see above). Each frame was acquired every 500 ms for 2 to 3 minutes. Calcium trace analysis was performed using Delta F up plugin (WCIF image J plugin) under Image J software. Individual cells corrected fluorescent intensity oscillation were then plotted with Origin 6 software. In some experiments, 10 μM MK801 or 1 μM TTX was flown, during acquisition, in the striatal compartment.

Quantification of axonal projections

After fixation and immuno-staining of axonal tubulin (β3-tubulin), whole chip images were captured at 400× magnification using the stitching function of Metamorph software (Molecular Imaging). Due to the high capacity of cortical axons to form axonal collaterals, the number of axons invading the receiving (or emitting) chambers was estimated by manually counting individual axon exiting each micro-channel at a distance of 50 μm from the exit of the micro-channel. This gives an estimation of the number of axons entering the chamber independent of their ramification. Selectivity of the diode design was estimated by comparing the number of axons exiting the micro-channels when cortical neurons were seeded at same density on the emitting or the receiving sides 8 days after seeding.

Statistical analysis

For morphological and phosphorylated ERK analyses, differences were assessed by an unpaired Student's *t* test from three independent experiments in which each experimental condition has been performed as a triplicate. For all analysis: * p-value < 0.05; ** p-value < 0.01; *** p-value < 0.001.

Author contributions

JMP invented the diode design, performed the initial neuronal network reconstruction, calcium analysis and wrote the paper. BD performed neuronal network reconstruction, characterization and wrote the paper. LS contributed to the diode design and MV performed the microfabrication experiments. SM and MP performed some cortical cultures. SB initiated the striatal cultures protocol. PVH performed calcium analysis and JC designed the pERK experiment. JLV supervised the microfluidic work and BB supervised the biological work.

Acknowledgements

The ANR Neuroscience research grant, "Plan Alzheimer" and the Fondation de France partly funded this project. PhD fellowships from Ministère de l'Enseignement Supérieur et de la Recherche to BD, SM, MV, and from Institut National du Cancer to LS are gratefully acknowledged.

References

1 E. W. Young and D. J. Beebe, Fundamentals of microfluidic cell culture in controlled microenvironments, *Chem. Soc. Rev.*, 2010, **39**, 1036–1048.
2 J. W. Park, B. Vahidi, A. M. Taylor, S. W. Rhee and N. L. Jeon, Microfluidic culture platform for neuroscience research, *Nat. Protoc.*, 2006, **1**, 2128–2136.
3 A. M. Taylor, M. Blurton-Jones, S. W. Rhee, D. H. Cribbs and C. W. Cotman, et al. A microfluidic culture platform for CNS axonal injury, regeneration and transport, *Nat. Methods*, 2005, **2**, 599–605.
4 J. Wang, L. Ren, L. Li, W. Liu and J. Zhou, et al. Microfluidics: a new cosset for neurobiology, *Lab Chip*, 2009, **9**, 644–652.
5 A. M. Taylor, D. C. Dieterich, H. T. Ito, S. A. Kim and E. M. Schuman, Microfluidic local perfusion chambers for the visualization and manipulation of synapses, *Neuron*, 2010, **66**, 57–68.
6 C. R. Gerfen, The neostriatal mosaic: multiple levels of compartmental organization in the basal ganglia, *Annu. Rev. Neurosci.*, 1992, **15**, 285–320.
7 A. C. Kreitzer, Physiology and pharmacology of striatal neurons, *Annu. Rev. Neurosci.*, 2009, **32**, 127–147.
8 H. Francisco, B. B. Yellen, D. S. Halverson, G. Friedman and G. Gallo, Regulation of axon guidance and extension by three-dimensional constraints, *Biomaterials*, 2007, **28**, 3398–3407.
9 N. Li and A. Folch, Integration of topographical and biochemical cues by axons during growth on microfabricated 3-D substrates, *Exp. Cell Res.*, 2005, **311**, 307–316.
10 V. Sgambato, C. Pagès, M. Rogard, M. J. Besson and J. Caboche, Extracellular signal-regulated kinase (ERK) controls immediate early gene induction on cortico striatal stimulation, *J. Neurosci.*, 1998, **18**, 8814–8825.
11 S. Pautot, C. Wyart and E. Y. Isacoff, Colloid-guided assembly of oriented 3D neuronal networks, *Nat. Methods*, 2008, **5**, 735–740.
12 O. Feinerman, A. Rotem and E. Moses, Reliable neuronal logic devices from patterned hippocampal cultures, *Nat. Phys.*, 2008, **4**, 967–973.
13 W. Tonomura, H. Moriguchi, Y. Jimbo and S. Konishi, Parallel multipoint recording of aligned and cultured neurons on corresponding Micro channel array toward on-chip cell analysis, *Conf Proc. IEEE Eng. Med. Biol. Soc.*, 2008, 943–946.
14 Y. Mourzina, D. Kaliaguine, P. Schulte and A. Offenhausser, Patterning chemical stimulation of reconstructed neuronal networks, *Anal. Chim. Acta*, 2006, **575**, 281–289.
15 A. E. Kincaid, T. Zheng and C. J. Wilson, Connectivity and convergence of single corticostriatal axons, *J. Neurosci.*, 1998, **18**, 4722–4731.
16 M. Matamales, J. Bertran-Gonzalez, L. Salomon, B. Degos, J. M. Deniau, E. Valjent, D. Hervé and J. A. Girault, Striatal medium-sized spiny neurons: identification by nuclear staining and study of neuronal subpopulations in BAC transgenic mice, *PLoS One*, 2009, **4**, e4770.
17 M. Segal, V. Greenberger and E. Korkotian, Formation of dendritic spines in cultured striatal neurons depends on excitatory afferent activity, *Eur. J. Neurosci.*, 2003, **12**, 2573–2585.
18 R. T. FremeauJr, S. Voglmaier, R. P. Seal and R. H. Edwards, VGLUTs define subsets of excitatory neurons and suggest novel roles for glutamate, *Trends Neurosci.*, 2004, **27**, 98–103.
19 T. Arendt, Synaptic degeneration in Alzheimer's disease, *Acta Neuropathol.*, 2009, **118**, 167–179.
20 G. R. Mallucci, Prion neurodegeneration: starts and stops at the synapse, *Prion*, 2009, **3**, 195–201.
21 R. Smith, P. Brundin and J. Y. Li, Synaptic dysfunction in Huntington's disease: a new perspective, *Cell. Mol. Life Sci.*, 2005, **62**, 1901–1912.
22 A. K. Hadjantonakis, M. Gertsenstein, M. Ikawa, M. Okabe and A. Nagy, Generating green fluorescent mice by germline transmission of green fluorescent ES cells, *Mech. Dev.*, 1998, **76**, 79–90.